Single-Molecule Magnet under dc field with Anion Effect: Self-Assembly of Pure Dysprosium(III) Metallacycles

Jianfeng Wu, Qianqian Yang, Haoyu Wang, Yan Ge, Jinkui Tang and Zhenhui Qi**

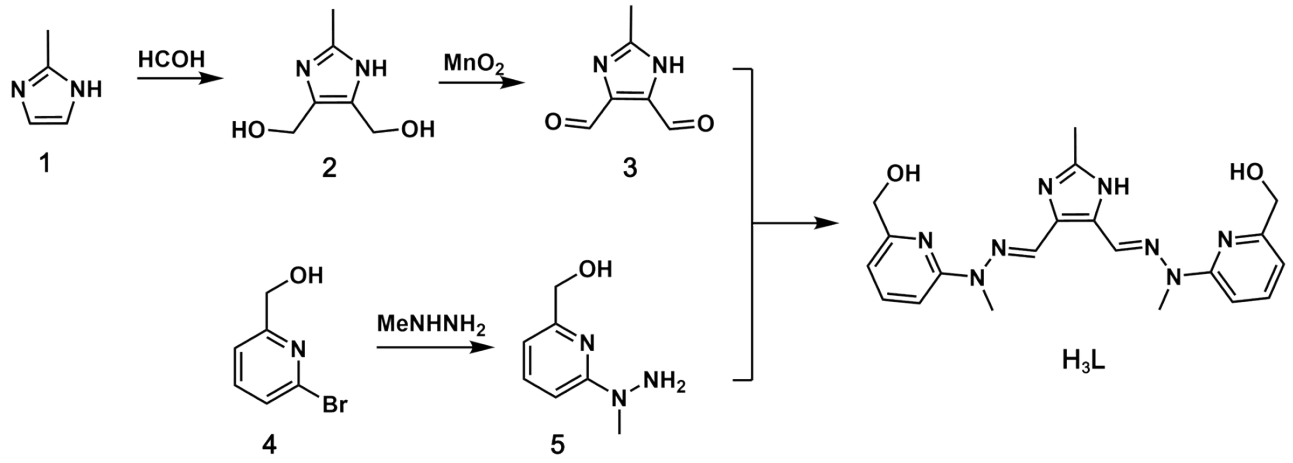

Scheme S1. Schematic drawing of the synthetic route of ligand **H_3L**.

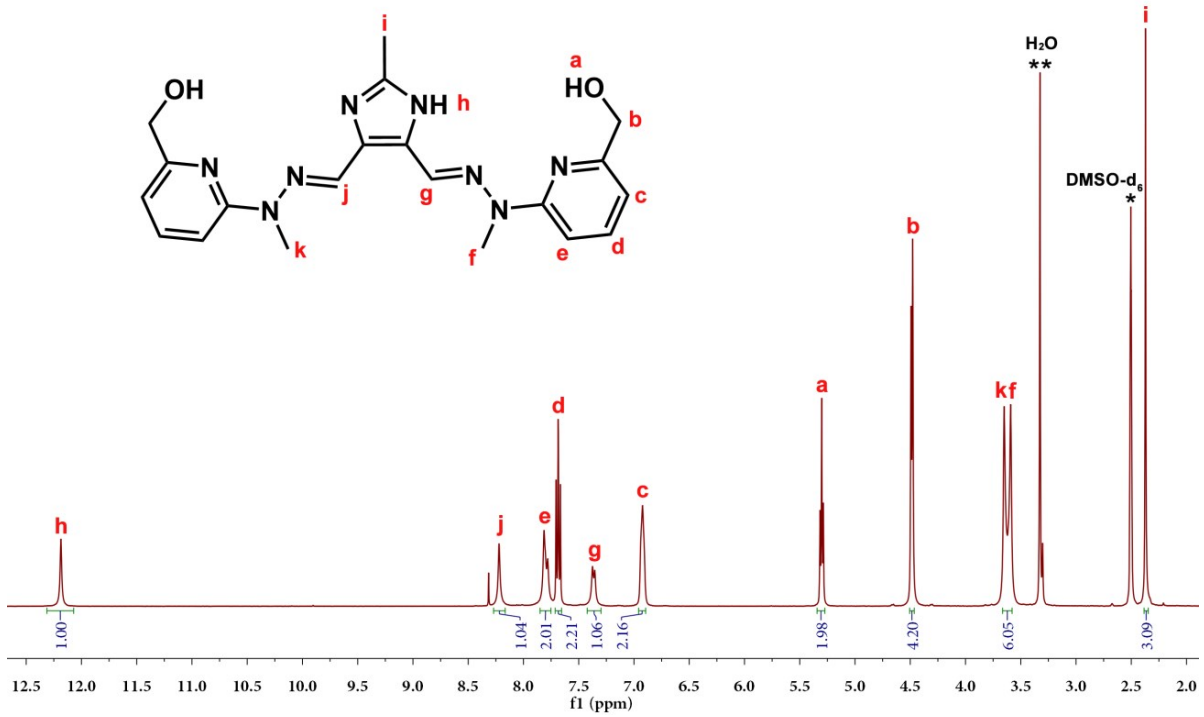

Fig. S1. ^{1}H-NMR spectrum of **H_3L** in DMSO-d_6 recorded at room temperature. Solvent peaks are marked with asterisks (DMSO-d_6, *; H_2O, **).

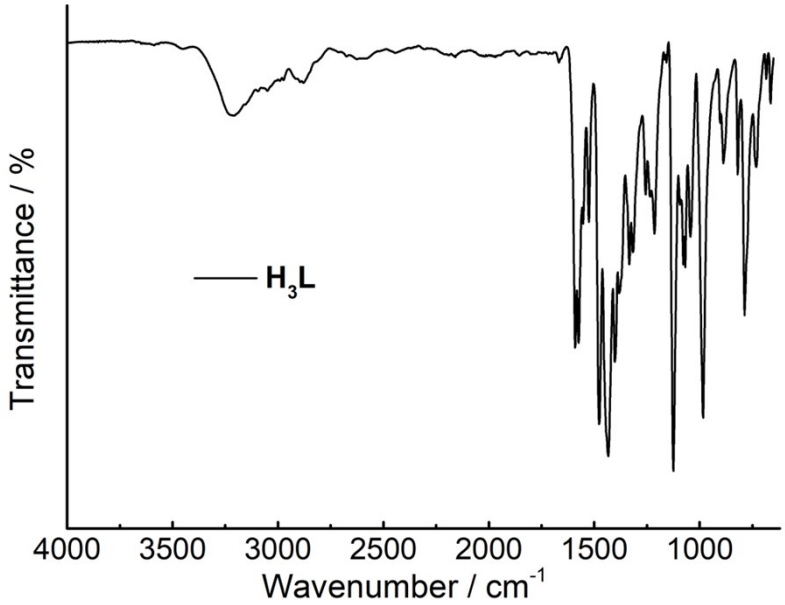

Fig. S2. IR (ATR) spectrum of solid sample for ligand **H_3L**.

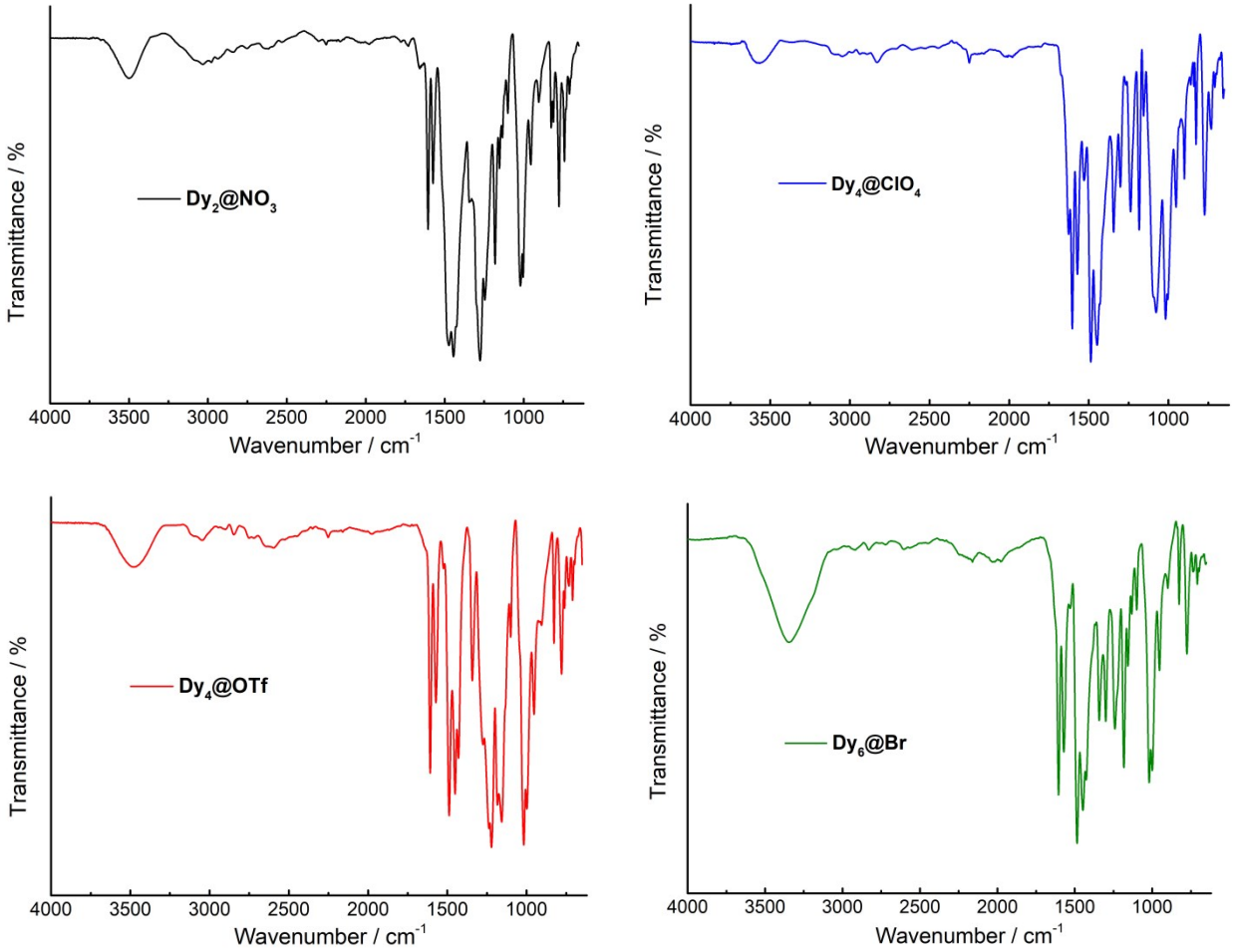

Fig. S3. IR (ATR) spectra of solid samples for complexes **Dy_2@NO_3**, **Dy_4@ClO_4**, **Dy_4@OTf**, and **Dy_6@Br**.

Table S1. Crystallographic data of complexes **Dy_2@NO_3**, **Dy_4@ClO_4**, **Dy_4@OTf**, and **Dy_6@Br**.

	Dy_2@NO_3	**Dy_4@ClO_4**	**Dy_4@OTf**	**Dy_6@Br**
empirical formula	$C_{25.77}H_{37.23}Dy_2N_{14.77}O_{19.23}$	$C_{80}H_{114}Cl_8Dy_4N_{32}O_{51}$	$C_{92}H_{101}Dy_4F_{24}N_{34}O_{34}S_8$	$C_{134}H_{212}Br_{12}Dy_6N_{48}O_{35}$
formula weight, g·mol^{-1}	1186.63	3273.63	3583.54	4989.42
crystal size, mm³	0.18 × 0.16 × 0.15	0.18 × 0.18 × 0.18	0.18 × 0.18 × 0.17	0.17 × 0.16 × 0.15
crystal system	Triclinic	Cubic	Monoclinic	Monoclinic
space group	*P*-1	*Pm-3n*	*C2/c*	*P21/n*
T, K	173.0	200.0	173.0	173.0
λ, Å	1.54178	1.54178	1.54178	1.54178
a, Å	11.6126(3)	26.8985(3)	25.3943(8)	20.2137(6)
b, Å	13.7845(4)	26.8985(3)	26.5959(9)	23.1408(7)
c, Å	14.7071(4)	26.8985(3)	43.3898(14)	21.4891(5)
α, °	63.1760(10)	90	90	90
β, °	88.7940(10)	90	96.012(2)	104.615(2)
γ, °	79.8230(10)	90	90	90
V, Å^3	2063.23(10)	19461.8(7)	29143.6(16)	9726.5(5)
Z	2	6	8	2
ρ (cal), g·cm^{-3}	1.910	1.676	1.633	1.704
F(000)	1162.0	9756.0	14144.0	4896.0
2*θ* range [°]	6.75 to 133.356	4.646 to 124.666	4.096 to 117.856	5.714 to 118.156
T_{max} / T_{min}	0.069 / 0.050	0.141 / 0.074	0.189 / 0.113	0.134 / 0.096
measured refl.	23881	57622	91507	63917
unique refl. [R_{int}]	7259, 0.0614	2781, 0.0728	20529, 0.0527	13874, 0.1007
goodness-of-fit (F^2)	1.044	1.213	1.045	1.034
data / restr. / param.	7259 / 19 / 587	2781 / 361 / 229	20521 / 527 / 1912	13874 / 79 / 984
*R*1, *wR*2 ($I > 2\sigma(I)$)	0.0395, 0.0983	0.1058, 0.2874	0.0667, 0.1837	0.0918, 0.2311
*R*1, *wR*2 (all data)	0.0473, 0.1048	0.1119, 0.2915	0.0765, 0.1919	0.1303, 0.2588
res. el. dens. [e·Å^{-3}]	0.86 / -1.64	2.00 / -2.24	2.49 / -1.75	3.15 / -3.02

Table S2. Selected bond distances (Å) and angles (°) in complex **Dy_2@NO_3**.

Dy1-O2	2.368(4)	Dy2-O1	2.378(4)	O2-Dy1-N8	65.15(14)	O1-Dy2-O17	69.26(13)
Dy1-O3	2.365(4)	Dy2-O10	2.429(4)	O3-Dy1-O2	75.99(14)	O1-Dy2-N1	64.18(13)
Dy1-O4	2.469(4)	Dy2-O11	2.477(4)	O3-Dy1-N5	98.79(15)	O16-Dy2-O17	50.12(12)
Dy1-O5	2.443(4)	Dy2-O13	2.466(4)	N5-Dy1-N6	67.04(14)	N1-Dy2-N3	62.28(14)
Dy1-O7	2.408(4)	Dy2-O14	2.502(4)	N6-Dy1-N8	61.89(14)	N4-Dy2-O16	72.75(14)
Dy1-O8	2.448(4)	Dy2-O16	2.515(4)	O5-Dy1-O8	149.65(15)	N4-Dy2-N3	66.48(14)
Dy1-N5	2.462(4)	Dy2-O17	2.534(4)	O7-Dy1-O4	153.32(16)	N4-Dy2-N12	75.40(15)
Dy1-N6	2.491(4)	Dy2-N1	2.479(4)	O7-Dy1-O5	142.35(15)	O10-Dy2-O13	134.78(13)
Dy1-N8	2.500(4)	Dy2-N3	2.532(4)	O8-Dy1-O4	130.68(15)	O10-Dy2-O14	149.14(13)
		Dy2-N4	2.454(4)			O11-Dy2-O14	134.84(13)
Dy1-Dy2	7.1238(5)					O13-Dy2-O11	161.58(14)

Table S3. Selected bond distances (Å) and angles (°) in complex **Dy_4@ClO_4**.

Dy1-O1	2.299(9)	O1#-Dy1-N3	76.2(3)
Dy1-O1#	2.299(9)	O1-Dy1-N4#	87.4(3)
Dy1-N3	2.506(10)	O1-Dy1-N1#	84.0(7)
Dy1-N3#	2.506(10)	O1-Dy1-N1	66.9(3)
Dy1-N4#	2.494(9)	N4-Dy1-N3#	87.0(3)
Dy1-N4	2.494(9)	N4-Dy1-N3	66.7(3)
Dy1-N1	2.477(5)	N4#-Dy1-N4	87.7(4)
Dy1-N1#	2.477(11)	N1-Dy1-N3	62.3(3)
Dy1-Dy1#	7.2475(8)	N1-Dy1-N4#	86.5(3)

1/2-Y, 1/2-X, 1/2-Z

Table S4. Selected bond distances (Å) and angles (°) in complex **Dy_4@CF_3SO_3**.

Dy1-O1	2.326(7)	Dy2-O6	2.328(7)	Dy3-O4	2.333(7)	Dy4-O2	2.391(6)
Dy1-O8	2.314(8)	Dy2-O7	2.318(7)	Dy3-O5	2.336(7)	Dy4-O3	2.410(6)
Dy1-N1	2.490(8)	Dy2-N21	2.444(8)	Dy3-N13	2.452(7)	Dy4-O9	2.529(6)
Dy1-N3	2.478(8)	Dy2-N22	2.464(8)	Dy3-N14	2.487(8)	Dy4-N5	2.494(8)
Dy1-N4	2.436(7)	Dy2-N24	2.459(8)	Dy3-N16	2.469(8)	Dy4-N6	2.467(8)
Dy1-N29	2.465(8)	Dy2-N25	2.459(8)	Dy3-N17	2.486(7)	Dy4-N8	2.485(8)

Dy1-N30	2.485(8)	Dy2-N27	2.456(8)	Dy3-N19	2.472(7)	Dy4-N9	2.482(8)
Dy1-N32	2.491(9)	Dy2-N28	2.446(8)	Dy3-N20	2.449(8)	Dy4-N11	2.456(8)
						Dy4-N12	2.526(7)
Dy1-Dy2	7.1754(8)	Dy2-Dy3	7.1347(8)	Dy3-Dy4	7.2275(8)	Dy4-Dy1	7.0968(8)
O1-Dy1-N1	66.4(3)	O6-Dy2-N21	87.6(3)	O4-Dy3-N16	66.2(3)	O2-Dy4-O9	69.5(2)
O1-Dy1-N30	73.9(3)	O6-Dy2-N22	74.2(3)	O4-Dy3-N17	77.6(3)	O2-Dy4-N8	66.0(2)
O1-Dy1-N32	85.9(3)	O6-Dy2-N24	78.1(3)	O4-Dy3-N19	75.5(3)	O2-Dy4-N11	70.4(2)
O8-Dy1-N1	80.3(3)	O6-Dy2-N25	66.7(3)	O4-Dy3-N20	87.2(3)	O2-Dy4-N12	74.7(2)
O8-Dy1-N3	76.4(3)	O7-Dy2-N24	66.0(3)	O5-Dy3-N14	77.1(2)	O3-Dy4-O9	70.1(2)
O8-Dy1-N4	87.9(3)	O7-Dy2-N25	82.8(3)	O5-Dy3-N16	77.7(3)	O3-Dy4-N5	72.3(2)
O8-Dy1-N32	65.3(3)	O7-Dy2-N27	74.6(3)	O5-Dy3-N17	65.6(2)	O3-Dy4-N6	68.8(2)
N3-Dy1-N1	62.8(3)	O7-Dy2-N28	88.6(3)	N13-Dy3-N14	67.5(2)	O3-Dy4-N9	65.5(2)
N4-Dy1-N3	67.8(2)	N21-Dy2-N22	68.3(3)	N13-Dy3-N19	88.1(2)	N5-Dy4-N12	77.4(2)
N4-Dy1-N29	85.4(2)	N21-Dy2-N25	86.4(3)	N16-Dy3-N14	62.8(2)	N6-Dy4-N5	67.8(2)
N4-Dy1-N30	88.9(3)	N21-Dy2-N27	87.6(3)	N19-Dy3-N17	62.6(2)	N6-Dy4-N12	82.5(2)
N4-Dy1 N32	83.4(3)	N21-Dy2-N28	87.9(3)	N20-Dy3-N13	90.0(3)	N8-Dy4-O9	72.6(2)
N29-Dy1-N3	86.3(3)	N24-Dy2-N22	63.5(3)	N20-Dy3-N14	88.3(2)	N8-Dy4-N12	83.8(2)
N29-Dy1-N30	68.3(3)	N27-Dy2-N25	63.1(3)	N20-Dy3-N16	88.2(3)	N9-Dy4-O9	72.5(2)
N30-Dy1-N32	62.4(3)	N28-Dy2-N22	86.3(3)	N20-Dy3-N19	68.6(2)	N9-Dy4-N5	79.4(2)
		N28-Dy2-N27	69.2(2)			N11-Dy4-N5	81.7(2)
						N11-Dy4-N12	67.0(2)

Table S5. Selected bond distances (Å) and angles (°) in complex **Dy_6@Br**.

Dy1-O2	2.372(10)	Dy2-O4	2.337(10)	Dy3-O11	2.405(11)
Dy1-O3	2.390(9)	Dy2-O5	2.390(9)	Dy3-O6	2.387(9)
Dy1-O8	2.515(10)	Dy2-N13	2.401(6)	Dy3-O7	2.489(13)
Dy1-N6	2.485(13)	Dy2-N14	2.476(12)	Dy3-N31	2.490(13)
Dy1-N9	2.462(7)	Dy2-N16	2.470(6)	Dy3-N22	2.531(12)
Dy1-N11	2.491(12)	Dy2-N17	2.464(6)	Dy3-N11	2.49(7)
Dy1-N12	2.486(7)	Dy2-N19	2.496(12)	Dy3-N41	2.46(7)
Dy1-N5	2.490(6)	Dy2-N20	2.397(6)	Dy3-N21	2.494(6)
Dy1-N8	2.465(7)			Dy3-N24	2.514(6)
Dy1-Dy2	70595(14)	Dy2-Dy3	7.1075(12)	Dy3-Dy1	7.1742(13)
O2-Dy1-O8	68.5(4)	O4-Dy2-N16	66.2(3)	O11-Dy3-N22	71.1(4)

O2-Dy1-N11	69.1(4)	O4-Dy2-N19	72.3(4)	O11-Dy3-N11	64.7(18)
O2-Dy1-N12	74.1(4)	O4-Dy2-N20	90.3(4)	O11-Dy3-N21	73.8(4)
O2-Dy1-N8	65.8(4)	O5-Dy2-N13	88.2(3)	O11-Dy3-N24	74.2(3)
O3-Dy1-O8	67.3(4)	O5-Dy2-N14	76.4(4)	O6-Dy3-N31	70.4(4)
O3-Dy1-N6	69.6(4)	O5-Dy2-N16	79.8(3)	O6-Dy3-N11	72(2)
O3-Dy1-N9	66.6(3)	O5-Dy2-N17	67.1(3)	O6-Dy3-N24	64.7(3)
O3-Dy1-N5	73.2(3)	N13-Dy2-N14	68.0(3)	O7-Dy3-N21	65.9(4)
N6-Dy1-N5	68.1(3)	N16-Dy2-N14	63.0(3)	N31-Dy3-N11	62(2)
N9-Dy1-O8	74.3(3)	N17-Dy2-N19	62.3(3)	N41-Dy3-O7	68.4(5)
N9-Dy1-N11	63.0(3)	N20-Dy2-N19	67.8(3)	N41-Dy3-N31	66.4(19)
N12-Dy1-N11	67.1(3)			N41-Dy3-N24	76.8(15)
N8-Dy1-O8	70.5(4)			N21-Dy3-N22	65.5(3)
N8-Dy1-N6	62.5(4)			N24-Dy3-N22	61.9(3)

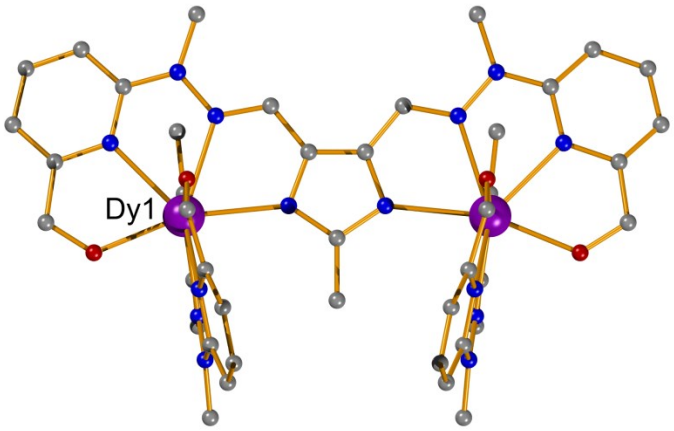

Fig. S4. Side view of the structure of complex **Dy_4@ClO_4**. The purple, gray, blue, and red spheres representing Dy, C, N, and O, respectively; hydrogen atoms, solvents, and free anions have been omitted for clarity.

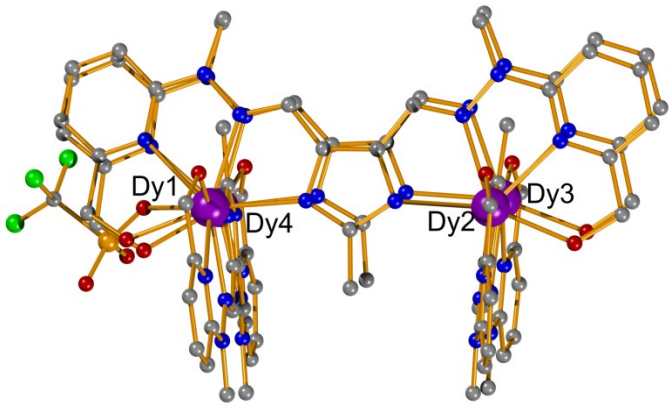

Fig. S5. Side view of the structure of complex **Dy_4@OTf**. The purple, green, orange, gray, blue, and red spheres representing Dy, F, S, C, N, and O, respectively; hydrogen atoms, solvents, and free anions have been omitted for clarity.

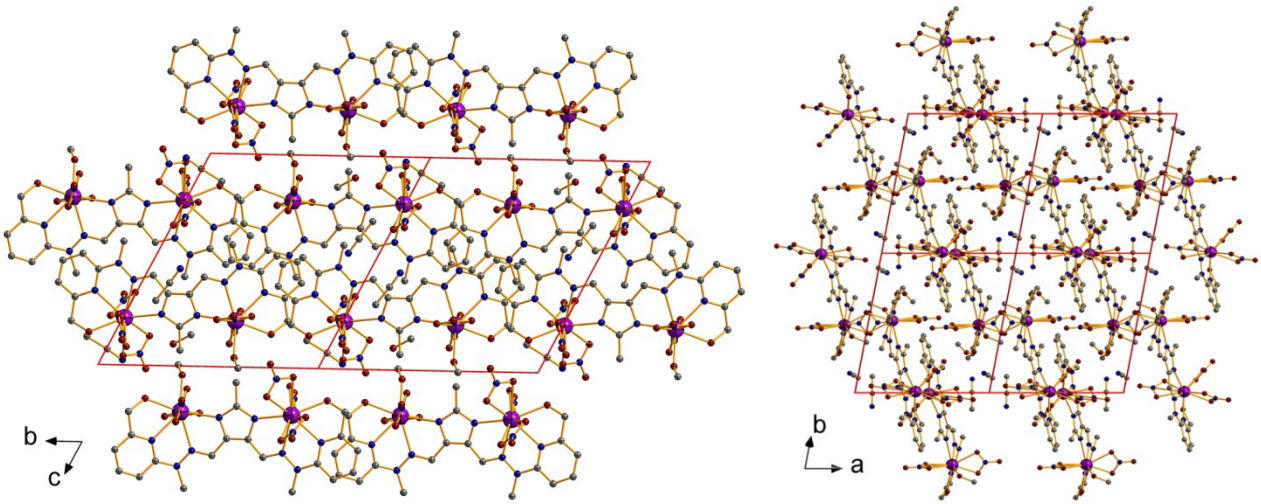

Fig. S6. Packing model along with *a* and *c* axes of complex **Dy_2@NO_3**. The purple, gray, blue, and red spheres representing Dy, C, N, and O, respectively; hydrogen atoms have been omitted for clarity.

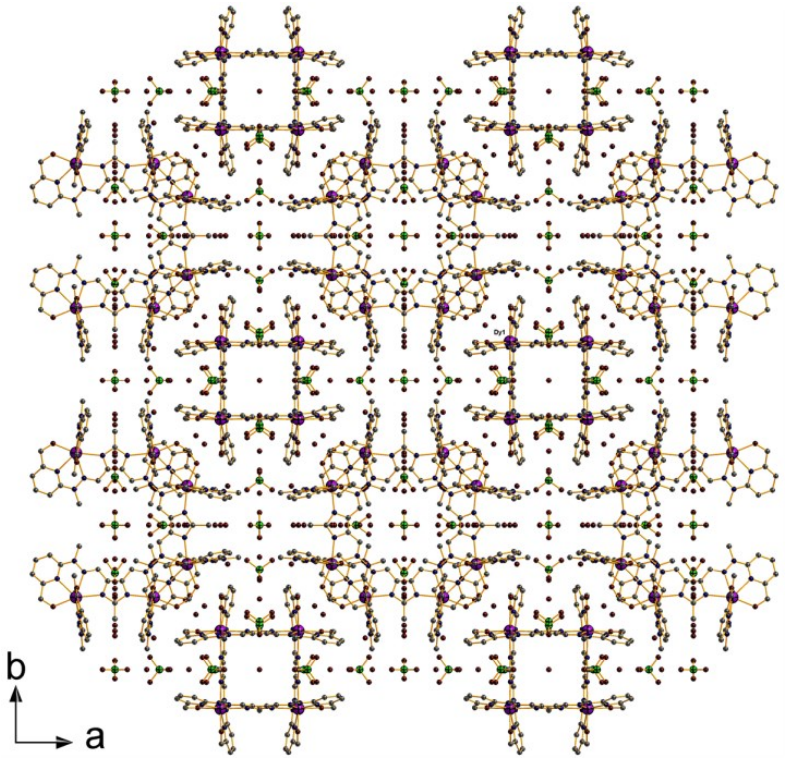

Fig. S7. Packing model along with *a* and *c* axes of complex **Dy_4@ClO_4**. The purple, green, gray, blue, and red spheres representing Dy, Cl, C, N, and O, respectively; hydrogen atoms have been omitted for clarity.

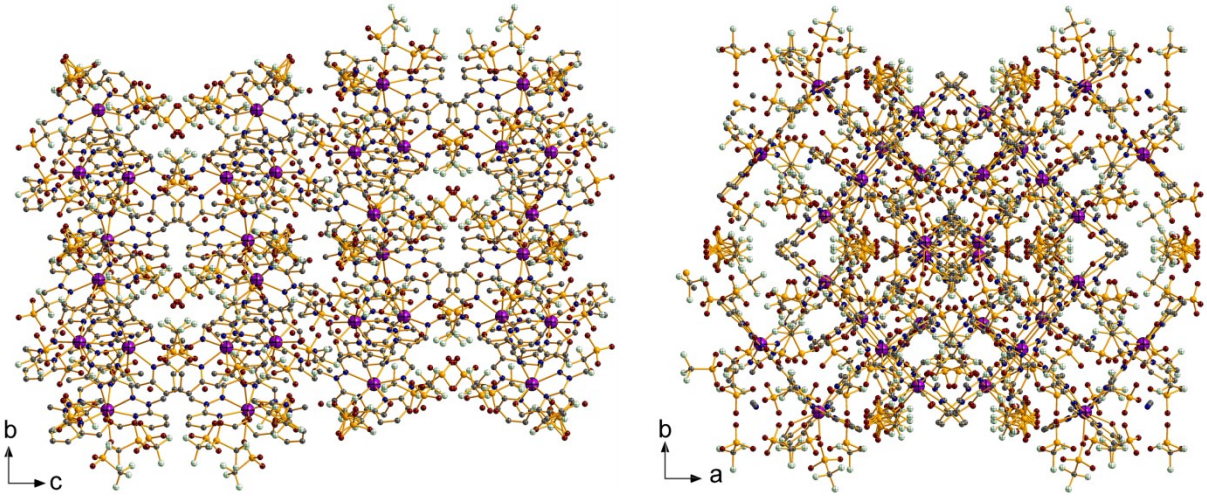

Fig. S8. Packing model along with *a* and *c* axes of complex **Dy_4@OTf**. The purple, orange, green, gray, blue, and red spheres representing Dy, S, F, C, N, and O, respectively; hydrogen atoms have been omitted for clarity.

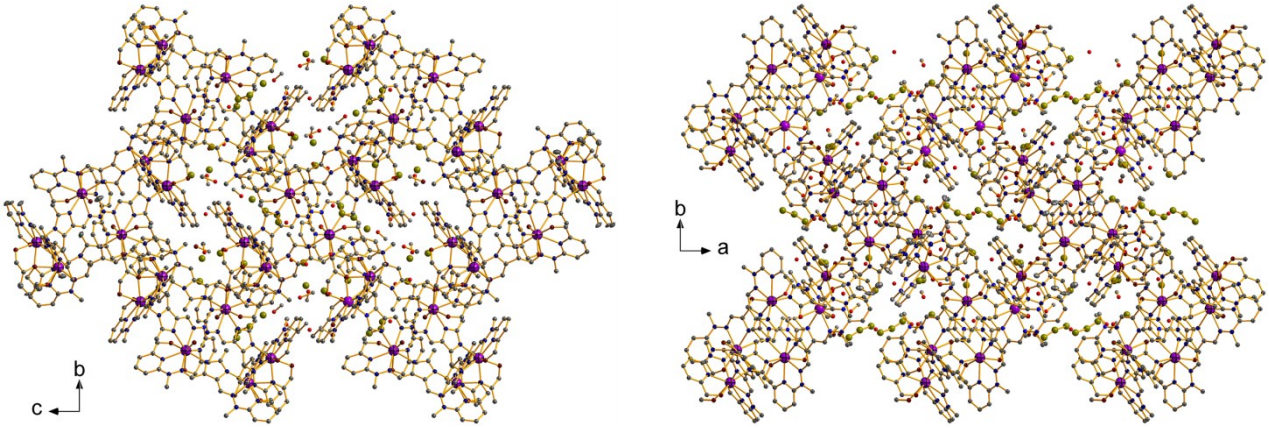

Fig. S9. Packing model along with *a* and *c* axes of complex **Dy_6@Br**. The purple, green, gray, blue, and red spheres representing Dy, Br, C, N, and O, respectively; hydrogen atoms have been omitted for clarity.

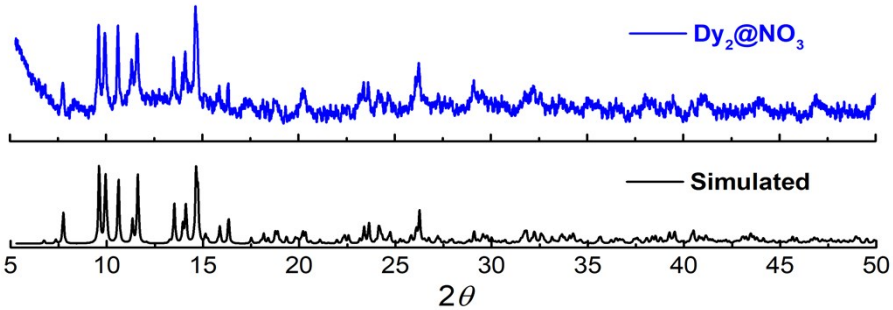

Fig. S10. Powder XRD analysis of complex **Dy_2@NO_3**. The black line is simulated data from single crystal data.

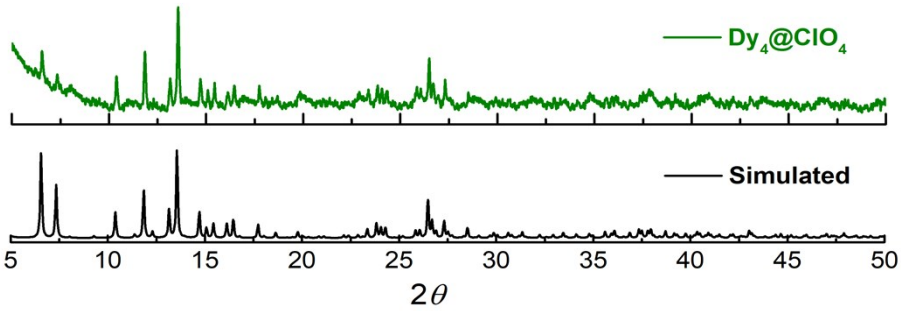

Fig. S11. Powder XRD analysis of complex **Dy_4@CO_4**. The black line is simulated data from single crystal data.

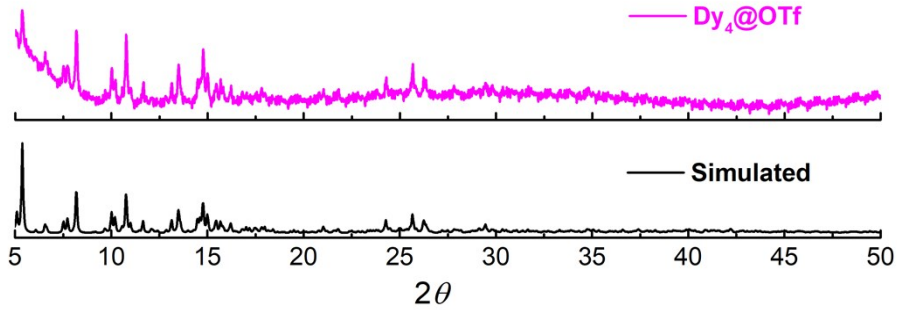

Fig. S12. Powder XRD analysis of complex **Dy_4@OTf**. The black line is simulated data from single crystal data.

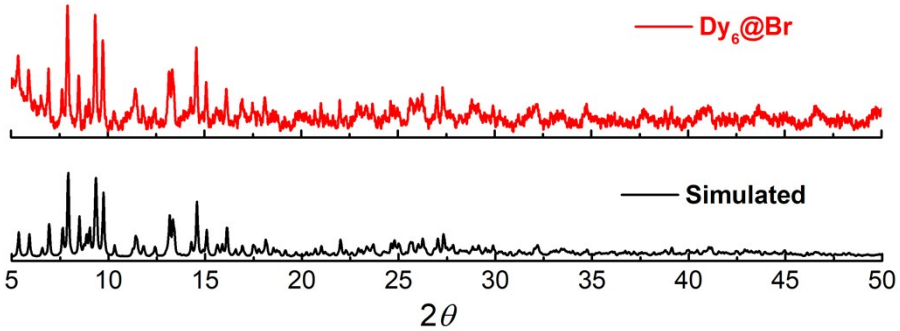

Fig. S13. Powder XRD analysis of complex **Dy_6@Br**. The black line is simulated data from single crystal data.

Table S6. The *CShM* values calculated by *SHAPE* 2.1[1] of Dy^{III} ions in **Dy_2@NO_3**.

Coordination Geometry	Dy1	Coordination Geometry	Dy2
Johnson triangular cupola (C_{3v})	12.851	Bicapped cube (D_{4h})	15.279
Capped cube (C_{4v})	13.849	Bicapped square antiprism (D_{4d})	9.692
Spherical-relaxed capped cube (C_{4v})	11.794	Bidiminished icosahedron (C_{2v})	10.879
Capped square antiprism (C_{4v})	8.179	Tridiminished icosahedron (C_{3v})	17.406
Spherical capped square antiprism (C_{4v})	7.026	Sphenocorona (C_{2v})	7.230
Tricapped trigonal prism (D_{3h})	8.141	Staggered Dodecahedron (D_2)	9.130
Spherical tricapped trigonal prism (D_{3h})	5.678	Tetradecahedron (C_{2v})	8.456

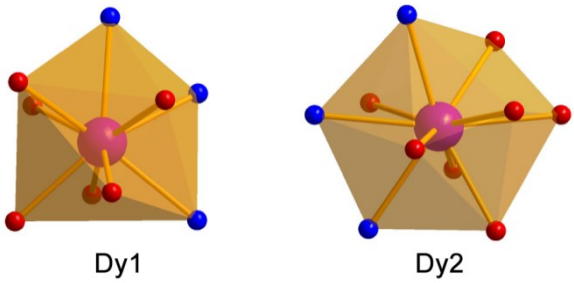

Fig. S14. Coordination polyhedrons of Dy1 (left) and Dy2 (right) in complex **Dy_2@NO_3**.

Table S7. The *CShM* values calculated by *SHAPE* 2.1 of Dy^{III} ion in **Dy_4@ClO_4**.

Coordination Geometry	Dy1
Cube (O_h)	11.246
Square antiprism (D_{4d})	5.425
Triangular dodecahedron (D_{2d})	3.357
Johnson gyrobifastigium J26 (D_{2d})	9.781
Elongated triangular bipyramid (D_{3h})	22.680
Biaugmented trigonal prism (C_{2v})	3.479
Snub diphenoid J84 (D_{2d})	3.489

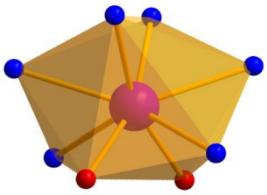

Fig. S15. Coordination polyhedron of Dy1 in complex **Dy_4@ClO_4**.

Table S8. The *CShM* values calculated by *SHAPE* 2.1 of Dy^{III} ions in **Dy_4@OTf**.

Coordination Geometry	Dy1	Dy2	Dy3	Coordination Geometry	Dy4
Cube (O_h)	14.736	14.784	14.348	Johnson triangular cupola (C_{3v})	18.829
Square antiprism (D_{4d})	9.619	9.177	9.241	Capped cube (C_{4v})	13.096
Triangular dodecahedron (D_{2d})	7.673	6.946	7.044	Spherical-relaxed capped cube (C_{4v})	12.809
Johnson gyrobifastigium J26 (D_{2d})	15.854	16.349	18.448	Capped square antiprism (C_{4v})	8.939
Elongated triangular bipyramid (D_{3h})	24.938	26.001	25.605	Spherical capped square antiprism (C_{4v})	6.446
Biaugmented trigonal prism (C_{2v})	9.037	8.466	8.374	Tricapped trigonal prism (D_{3h})	10.207
Snub diphenoid J84 (D_{2d})	11.424	10.612	11.191	Spherical tricapped trigonal prism (D_{3h})	6.062

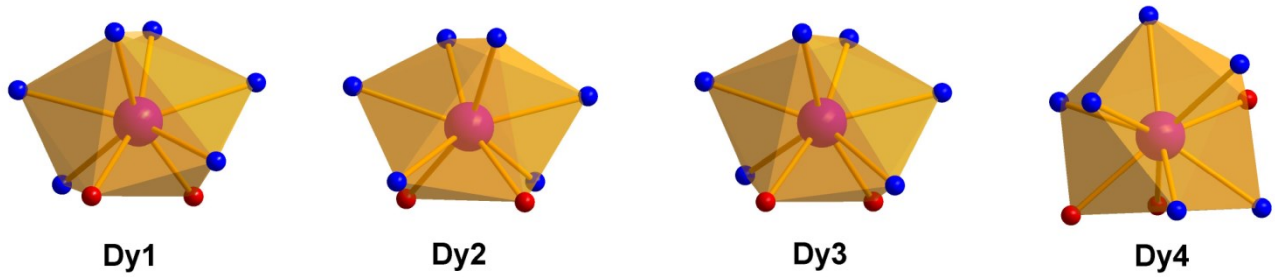

Fig. S16. Coordination polyhedrons of Dy1, Dy2, Dy3, and Dy4 in complex **Dy_4@OTf**.

Table S9. The *CShM* values calculated by *SHAPE* 2.1 of Dy^{III} ions in **Dy_6@Br**.

Coordination Geometry	Dy1	Dy3	Coordination Geometry	Dy2
Johnson triangular cupola (C_{3v})	15.309	13.722	Cube (O_h)	11.866
Capped cube (C_{4v})	9.634	7.827	Square antiprism (D_{4d})	6.899
Spherical-relaxed capped cube (C_{4v})	9.759	8.414	Triangular dodecahedron (D_{2d})	5.323
Capped square antiprism (C_{4v})	3.238	2.311	Johnson gyrobifastigium J26 (D_{2d})	11.647
Spherical capped square antiprism (C_{4v})	3.061	2.831	Elongated triangular bipyramid (D_{3h})	18.661
Tricapped trigonal prism (D_{3h})	3.822	3.857	Biaugmented trigonal prism (C_{2v})	5.292
Spherical tricapped trigonal prism (D_{3h})	3.814	3.389	Snub diphenoid J84 (D_{2d})	6.152

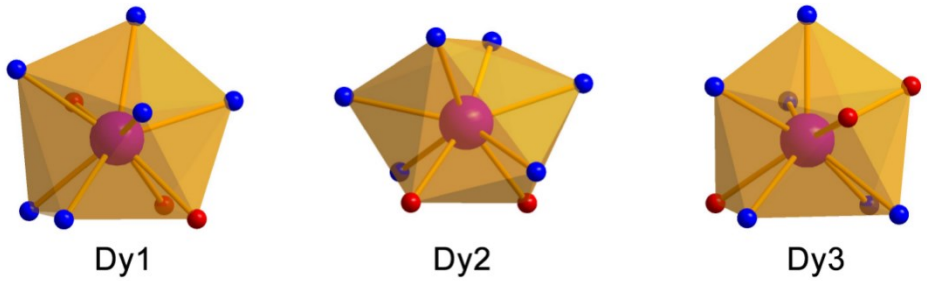

Fig. S17. Coordination polyhedrons of Dy1 (left), Dy2 (middle), and Dy3 (right) in complex **Dy_6@Br**.

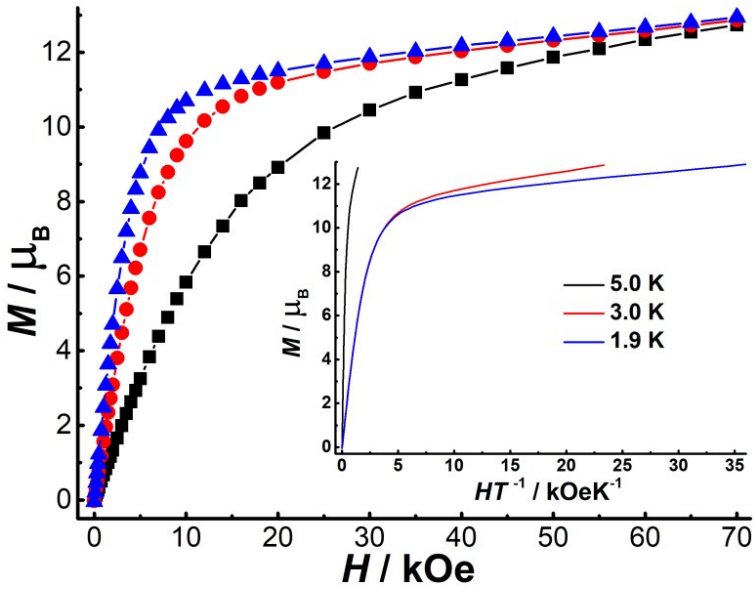

Fig. S18. Molar magnetization (*M*) *vs*. magnetic field (*H*) for **Dy_2@NO_3** at 1.9, 3.0, and 5.0 K. Inset represents the relevant plots of *M vs*. *H/T*.

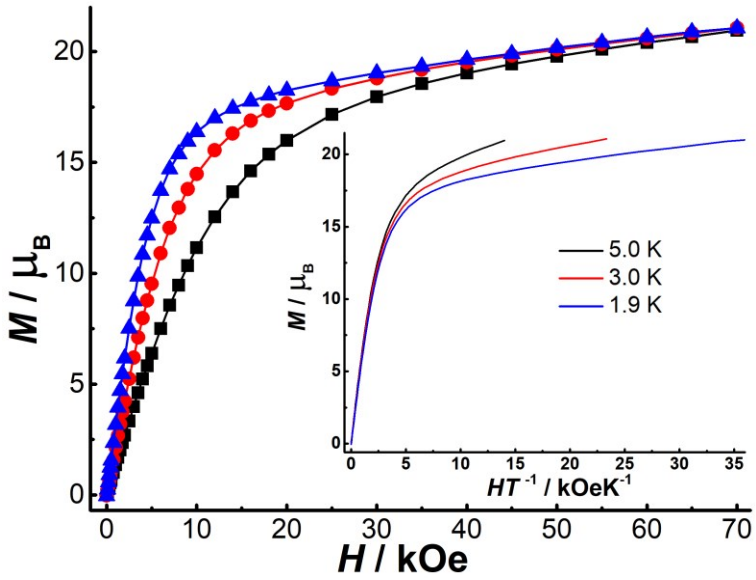

Fig. S19. Molar magnetization (*M*) *vs*. magnetic field (*H*) for **Dy_4@ClO_4** at 1.9, 3.0, and 5.0 K. Inset represents the relevant plots of *M vs*. *H/T*.

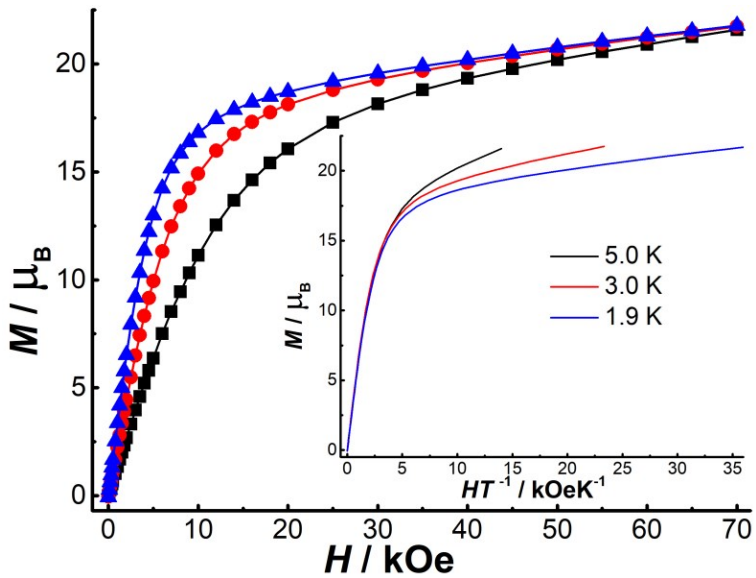

Fig. S20. Molar magnetization (*M*) *vs*. magnetic field (*H*) for **Dy_4@OTf** at 1.9, 3.0, and 5.0 K. Inset represents the relevant plots of *M vs*. *H/T*.

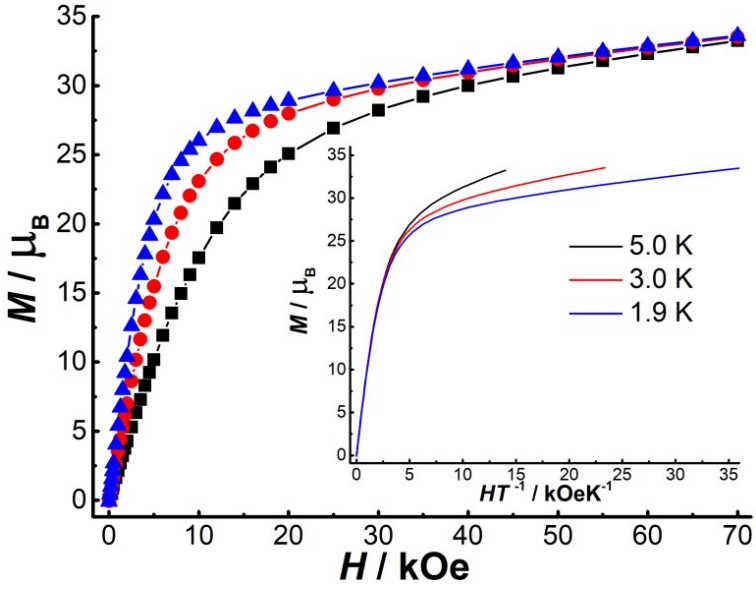

Fig. S21. Molar magnetization (*M*) *vs*. magnetic field (*H*) for **Dy_6@Br** at 1.9, 3.0, and 5.0 K. Inset represents the relevant plots of *M vs*. *H/T*.

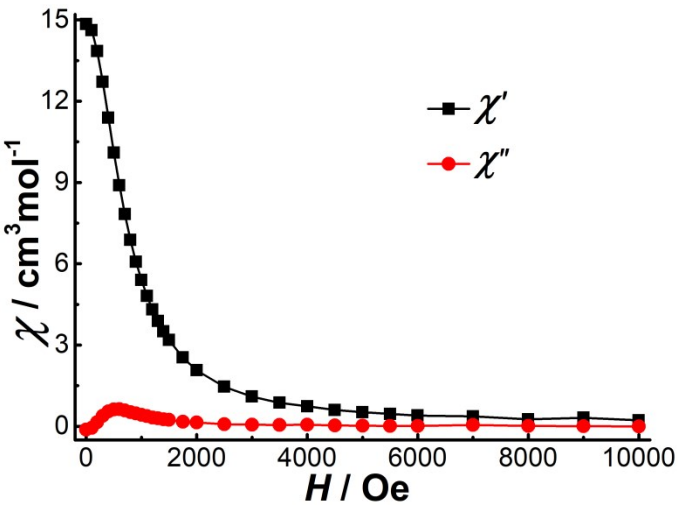

Fig. S22. Field-dependent ac susceptibility of **Dy_2@NO_3** at 1.9 K with ac frequency of 1488 Hz.

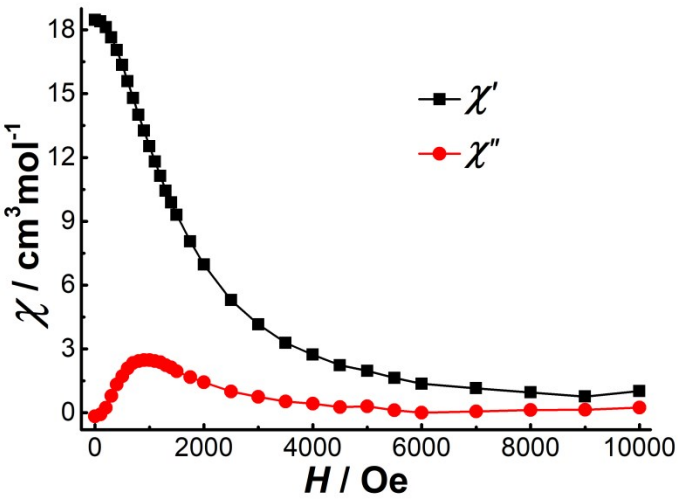

Fig. S23. Field-dependent ac susceptibility of **Dy_4@ClO_4** at 1.9 K with ac frequency of 1488 Hz.

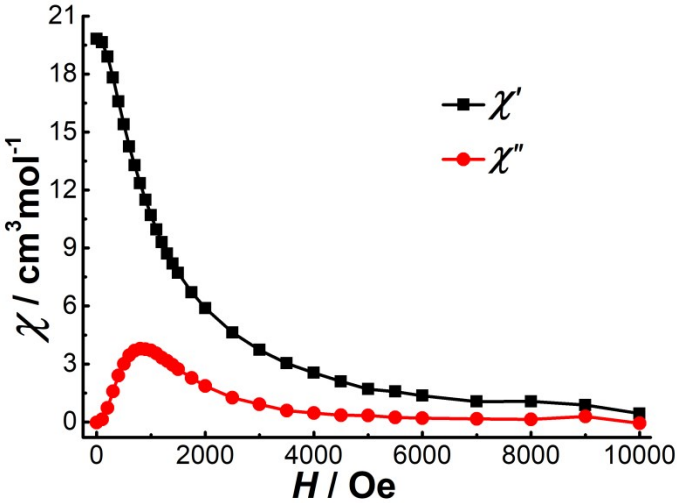

Fig. S24. Field-dependent ac susceptibility of **Dy_4@OTf** at 1.9 K with ac frequency of 1488 Hz.

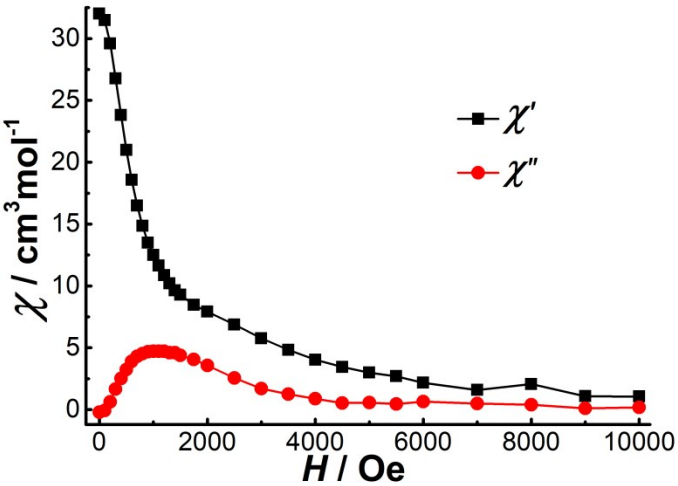

Fig. S25. Field-dependent ac susceptibility of **Dy_6@Br** at 1.9 K with ac frequency of 1488 Hz.

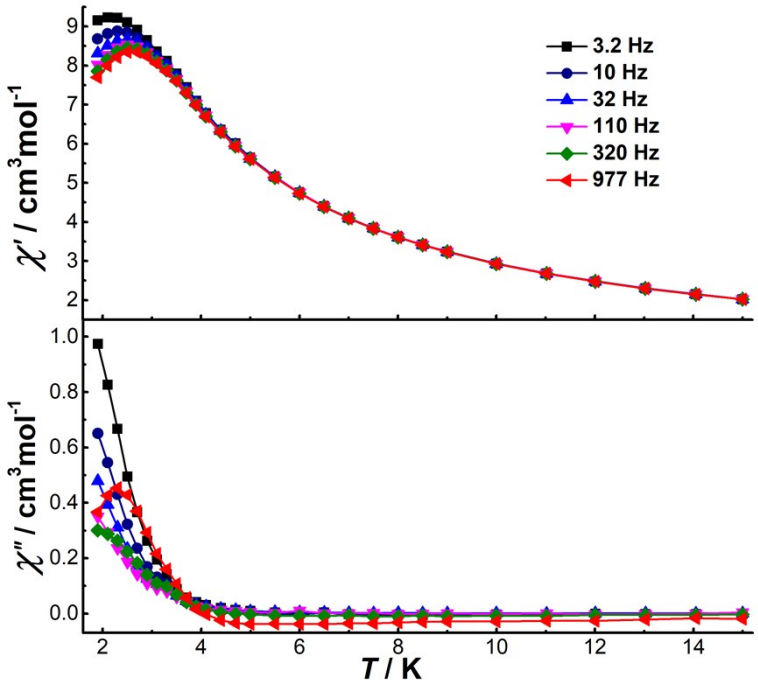

Fig. S26. Temperature-dependent ac susceptibility of **Dy_2@NO_3** under 600 Oe dc field.

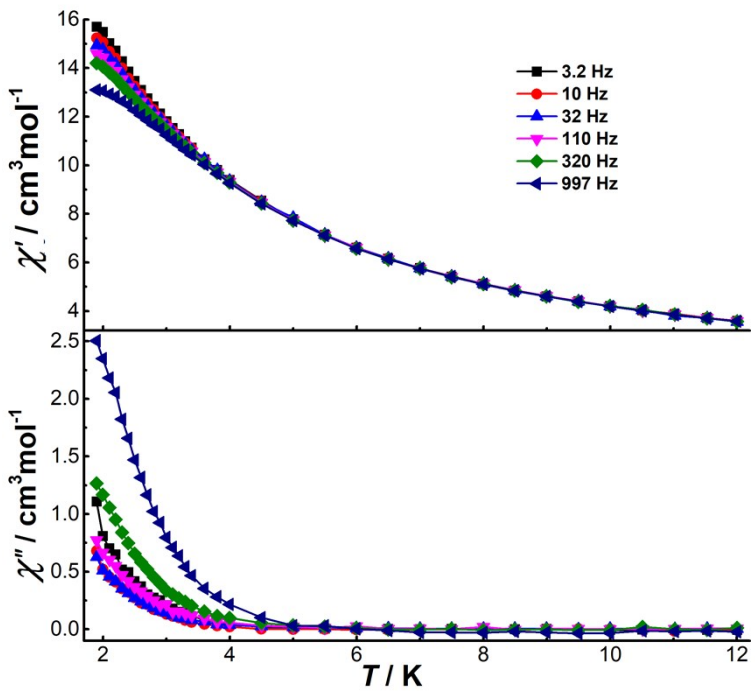

Fig. S27. Temperature-dependent ac susceptibility of **Dy_4@ClO_4** under 900 Oe dc field.

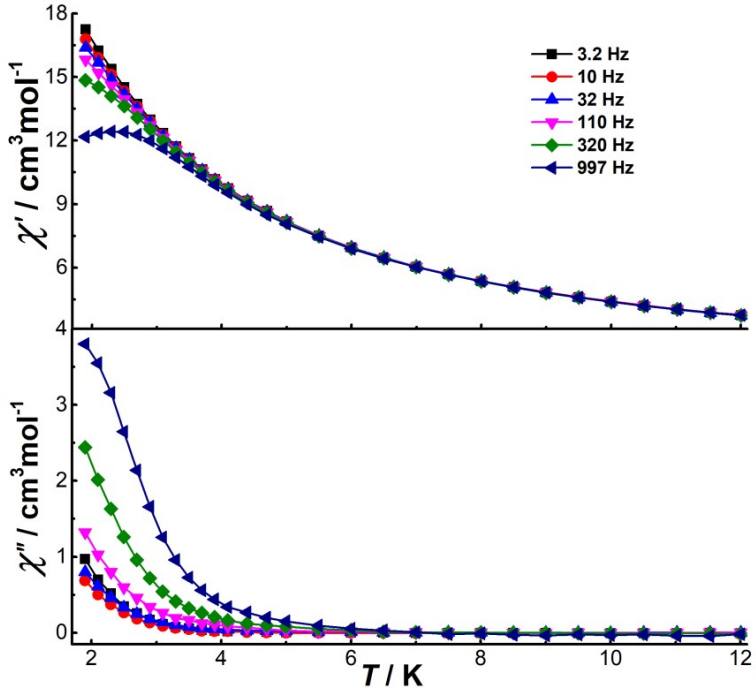

Fig. S28. Temperature-dependent ac susceptibility of **Dy_4@OTf** under 800 Oe dc field.

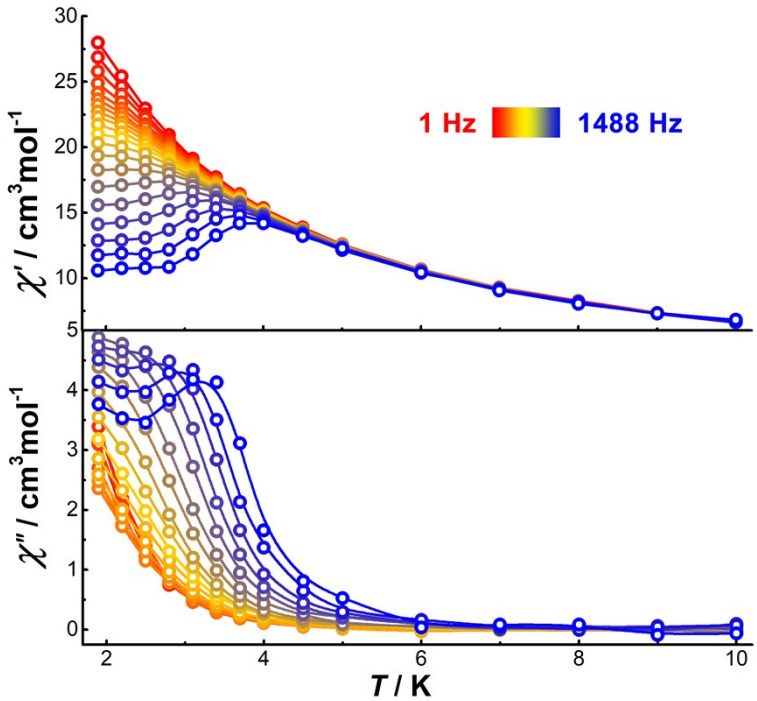

Fig. S29. Temperature-dependent ac susceptibility of **Dy_6@Br** under 1000 Oe dc field.

Table S10. The best fit of frequency-dependent ac susceptibility of **Dy_6@Br** under 1000 Oe dc field.

T / K	$\chi_{S,tot}$	$\Delta\chi_1$	τ_{1} / s	α_1	$\Delta\chi_2$	τ_{2} / s	α_2	*Residual*
1.9	6.08789	5.84561	0.10393	1.9868E-6	18.1719	4.44701E-4	0.38619	0.12304
2.2	7.22349	3.70182	0.09149	3.26219E-6	15.5654	4.12826E-4	0.3179	0.20437
2.5	7.64501	2.4193	0.07782	7.04635E-6	13.4717	3.2463E-4	0.25095	0.33566
2.8	7.34454	1.50084	0.05626	1.87413E-5	12.2512	2.16758E-4	0.20141	0.5056
3.1					11.87016	1.18794E-4	0.19483	0.46239
3.4					13.54823	4.61316E-5	0.21548	0.24974
3.7					16.0406	1.65038E-5	0.22512	0.18382
4					15.0833	7.00461E-6	0.26487	0.07383
4.5					13.662	2.20095E-6	0.3175	0.0314
5					12.47149	8.60445E-7	0.35885	0.05461

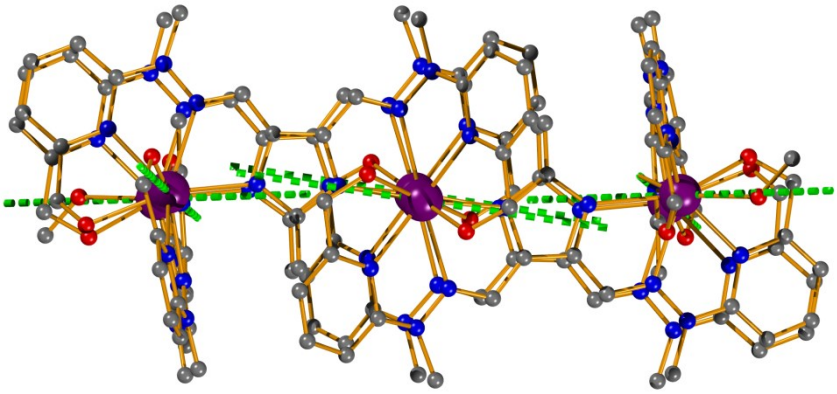

Fig. S30. Orientations of the main magnetic axes of the ground state for the Dy^{III} ions calculated based on the whole molecule of **Dy_6@Br**. The hydrogen atoms have been omitted for clarity.

Table S11. Minimal reorientation energies (cm^{-1}) and intersection angles (°) of the anisotropy axes calculated with Magellan program[2] for complex **Dy_6@Br**.

Site	Optimized energy (cm^{-1})	Min. reversal energy (cm^{-1})	Intersection angles (°)
Dy1	-0.1769E+03	0.1387E+03	0

Dy2	-0.1430E+03	0.9648E+02	36.715
Dy3	-0.3648E+03	0.4970E+03	62.966
Dy1'	-0.1769E+03	0.1387E+03	0
Dy2'	-0.1429E+03	0.9644E+02	36.715
Dy3'	-0.3648E+03	0.4970E+03	62.966

References:

1 a) S. Alvarez and M. Llunell, *J. Chem. Soc., Dalton Trans.*, 2000, 10.1039/B004878J, 3288-3303; b) D. Casanova, P. Alemany, J. M. Bofill and S. Alvarez, *Chem. Eur. J.*, 2003, **9**, 1281-1295.

2 N. F. Chilton, D. Collison, E. J. L. McInnes, R. E. P. Winpenny and A. Soncini, *Nat. Commun.*, 2013, **4**, 2551.